

3D FIELD-SCALE REACTIVE TRANSPORT MODELING OF IN SITU IMMOBILIZATION OF URANIUM IN STRUCTURED POROUS MEDIA VIA BIOSTIMULATION

YILIN FANG¹, TIMOTHY SCHEIBE¹, ERIC RODEN², WIWAT KAMOLPORNWIJIT¹
AND SCOTT BROOKS³

¹ Pacific Northwest National Laboratory, Richland, WA 99352, USA yilin.fang@pnl.gov;

² University of Wisconsin, Richland, WA 99352, USA; ³ Oak Ridge National Laboratory, Oak Ridge, TN 37831, USA

ABSTRACT

A several-month-long ethanol injection experiment is being conducted to study the impacts of porous media structure (i.e., heterogeneity existing at multiple scales) on the effectiveness of metal/radionuclide bioremediation in a highly heterogeneous unconfined aquifer near Oak Ridge, TN, USA. We have constructed a 3D field-scale groundwater flow and multicomponent reactive transport model to simulate the experimental observations. The model incorporates a suite of abiotic reactions and microbially-mediated redox reactions for multiple terminal electron accepting processes (TEAPs) including soluble oxygen, nitrate, U(VI) and sulfate and solid-phase electron acceptors. Different biomass populations are considered in the model. Growth of these populations is derived from the bioenergetics-based approach in which the partitioning of electron flow between energy generation and cell biomass production is dependent on the free energy of the corresponding TEAP. TEAP reaction rates were free energy constrained. The TEAP model and reaction system have been formulated and used to simulate laboratory batch experimental observations. We conducted the field-scale simulation starting with the reaction system and parameters obtained from the batch experiment and hydrologic parameters estimated from the results of pumping tests, water level monitoring and model interpretation of a tracer test conducted in August 2004. Reaction parameters were investigated to compare simulation results and field experiment observations.

1. INTRODUCTION

We are performing field-scale experiments in a highly heterogeneous unconfined aquifer near Oak Ridge, Tennessee. The groundwater and sediment contains contaminants including uranium, nitrate, and technetium. Our research focuses on an in situ field-scale biostimulation experiment to evaluate the feasibility of stimulating microbial U(VI) reduction activity in targeted pore fractions of structured porous media in the aquifer (Roden and Scheibe, 2005). The goal of biostimulation in this case is the in situ immobilization of uranium through precipitation of relatively insoluble U(IV) mineral phases. Geologic materials that comprise the surficial aquifer can be broadly lumped into three general classes (Figure 1): 1) underlying bedrock of the Nolichucky shale (shale with interbedded limestone), 2) undisturbed shale saprolite (highly weathered bedrock that has unconsolidated character but retains much of the bedding and fracture structure of the parent rock; Driese et al., 2001, McKay et al., 2005),

and 3) disturbed fill within a zone from which contaminated soils were historically excavated and replaced by unspecified materials (probably primarily native saprolite excavated from a nearby uncontaminated area). This material also contains a significant fraction of limestone gravel mixed with the disturbed saprolite throughout the fill interval. Examination of borehole cores from the area and results of hydraulic tests (pumping and tracer tests) indicate that there exists a highly conductive layer at the bottom of the disturbed fill zone in which gravel clasts are the dominant material. The highest uranium concentrations observed in sediment extractions from borehole cores occur in the intact saprolite and fill immediately below and above the coarse gravelly zone.

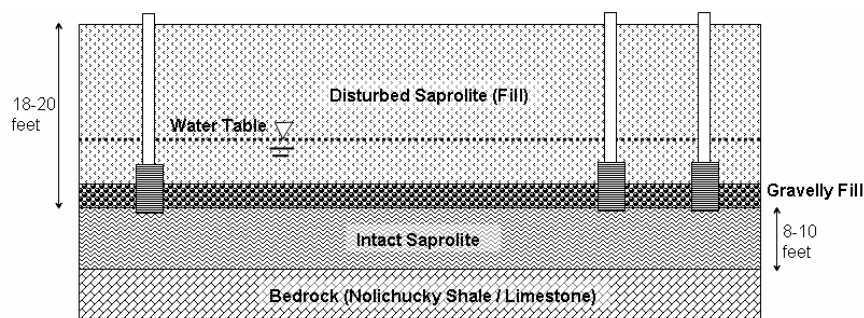


FIGURE 1. Schematic diagram of aquifer stratigraphy at the research area.

In late September 2005 a field-scale biostimulation experiment was initiated by injecting an ethanol solution (as an electron donor) into three wells (FW212, FW213, and FW214 in Figure 2). The hypotheses guiding the experiment are:

- 1) Injection of electron donor into the gravel layer will result in dispersive and diffusive mass transfer into the adjacent fill/saprolite zones. This will stimulate microbial activity at the interface between the gravel and fill/saprolite layers that will inhibit large-scale mass transfer of uranium into the gravel, thus reducing transport of uranium to downgradient receptor points (Figure 3).
- 2) Within the saprolite and fill zones immediately adjacent to the gravel, in which the electron donor levels can be maintained at sufficient levels, localized microbarriers will form around intact blocks of porous saprolite, thereby trapping uranium within the micropore domain (Roden and Scheibe, 2005).
- 3) Within the gravel, microbial activity will be stimulated in the fine-grained material and surface coatings surrounding gravel clasts, and will therefore create localized microbarriers around those clasts, thereby trapping uranium within the intragranular pore spaces. This activity will also reduce U(VI) dissolved in the groundwater flowing through the flow cell from upgradient sources, causing it to precipitate and become immobilized.

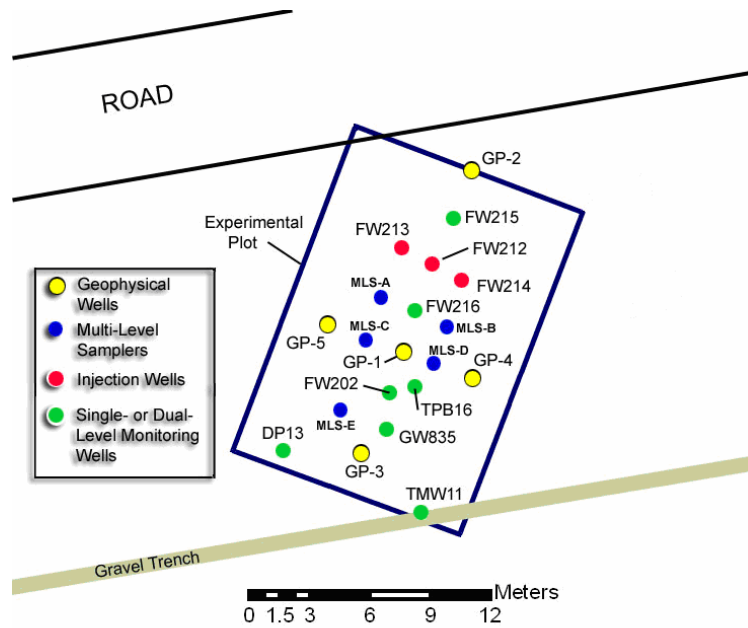


FIGURE 2. Schematic diagram of experimental plot layout. Injection wells are shown in red. Groundwater flow is from top to bottom in this figure, aligned with the long axis of the plot which is approximately from north to south.

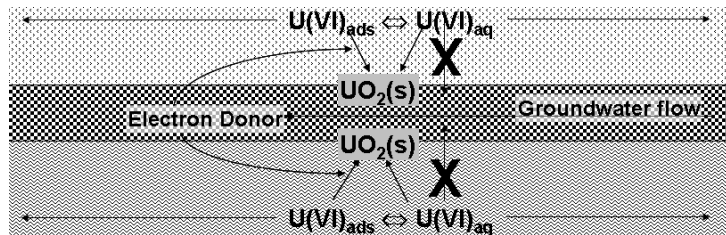


FIGURE 3. Immobilization of U(VI) at the interface between gravel zone and fill/saprolite zone

2. NUMERICAL SIMULATION OF FIELD EXPERIMENT

The numerical simulation is based on the injection strategy utilized in the field-scale biostimulation experiment. An initial 24-hour pulse of injection solution containing bromide and ethanol was used as a pre-injection tracer flush experiment (Scheibe et al., 2005) and to initiate microbial activity throughout the experimental zone. Subsequently, a 1-hour pulse of the bromide/ethanol solution has been injected each day (every 24 hours) to continue biostimulation at the desired level.

The hydrologic parameters and geometric structure of the numerical model were based on geological and geophysical characterizations of the site and on parameter estimation based on fitting to results of a bromide tracer test conducted in 2004.

The biogeochemical reaction system was based on batch experiments conducted using sediments from cores in the research area. Rate parameters for critical terminal electron accepting processes (TEAPs) were estimated by model fitting to laboratory observations. These rates and reaction system were directly applied to the field-scale model without modification (no fitting to field observations from the biostimulation experiment).

1.1 Conceptual model.

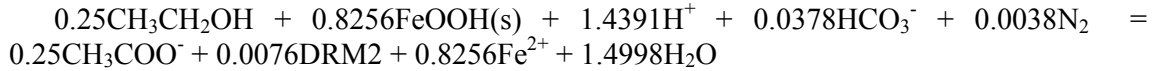
For the numerical simulation, we assume the water table is 4 meters below ground surface. The three-dimensional model domain comprises disturbed fill, coarse gravel, and intact saprolite zones as shown in Figure 1. The model domain is 20 meters long, 10 meters wide, and its saturated thickness is 4 meters. The bottom boundary, corresponding to intact bedrock of very low permeability, is treated as a no-flow boundary. Injection wells are screened over the interval between 4.5 m and 6 m depth. The model x-coordinate axis is aligned with the long axis of the flow cell (Figure 2), with $x=0$ corresponding to well FW215 and $y=0$ corresponding to the west edge of the flow cell. Well coordinates in meters are (2.5,3.3) for well FW214, (2.5, 5.0) for well FW212 and (2.5,6.7) for well FW213. The thicknesses and hydraulic properties of each layer are summarized in Table 1. Dispersivities were estimated by model fitting of a bromide tracer test conducted in 2004. Longitudinal dispersivity is 1.0 m, transverse dispersivity is 0.1 m. Horizontal discretization size of the numerical grid varies from 0.5 m to 2 m, and vertical discretization varies from 0.25 to 0.5 m.

TABLE 1. Geometric size and hydraulic properties of simulation domain

	Thickness (m)	Porosity	Hydraulic Conductivity (cm/s)
Disturbed Saprolite Fill	1.5	0.3	1.3×10^{-2}
Gravelly Fill	0.5	0.3	3.8×10^{-2}
Intact Saprolite	2.0	0.1	4.1×10^{-5}

1.2 Reaction model.

The TEAP (terminal electron accepting process) model of Roden et al. (2005) was converted to the reaction network form used by the reaction-based biogeochemical simulator BIOGEOCHEM (Fang et al., 2003, Fang et al., 2005) and transport model HYDROGEOCHEM (Yeh et al., 2005) for field-scale modeling of biostimulation at the research site. The TEAP model accounts for complete (to HCO_3^-) or incomplete (to acetate) oxidation of ethanol via 7 core TEAP pathways (see Table 2). Each of the TEAP reactions is dependent on the biomass of one or more distinct microbial populations chosen based on current knowledge of the kinds of organisms likely to be involved in ethanol metabolism. Thus a total of 29 TEAPs are considered in the model. Growth of these populations is described using the bioenergetics-based approach developed by Rittman and McCarty (2001) for simulation of wastewater (i.e. sewage) treatment, in which the partitioning of electron flow between energy generation and cell biomass production is dependent on the free energy of the corresponding TEAP. This approach alleviates the need for making a priori assumptions about the biomass yield for the different physiological functional populations. For example, the biomass yield for TEAP reaction (5) in Table 2 catalyzed by dissimilatory reducing microorganisms DRM2 can be derived to be $0.0076 \times 113 / 0.25 = 3.435$ g cells/mol ethanol from the following overall reaction obtained using bioenergetics-based approach:



Each of the TEAPs results in production of various inorganic compounds, which either accumulate in solution or undergo reactions (sorption and/or mineral precipitation) with the solid-phase. Using the TEAP model and a suite of abiotic reactions, Dr. Roden reproduced the basic patterns of organic substrate metabolism, consumption of electron acceptors (NO_3^- , Fe(III), SO_4^{2-}), and accumulation of reduced end-products (Fe(II) and CH_4) of anaerobic respiration in a slurry experiment with ethanol-amended subsurface sediment (Roden et al., 2005, Roden, 2005). The general agreement between the simulation and the slurry experiment data suggests that the developed reaction network is appropriate for incorporation into field-scale simulations of natural or engineered subsurface microbial processes.

The model contains a large number of parameters (see Roden et al., 2005). For example, in the rate formulation for Fe(III) reduction,

$$R_{\text{Fe(III)}} = \mu_{\text{max}} \frac{[\text{Cells}]}{K_{\text{m}_{\text{Cells}}} + [\text{Cells}]} [\text{Fe(III)}]_{\text{Surf}} f_{\text{Free}} f(\Delta G_{\text{rxn}}) \frac{K_{\text{m}_{\text{O}_2}}}{K_{\text{m}_{\text{O}_2}} + [\text{O}_2]} \frac{K_{\text{m}_{\text{NO}_3}}}{K_{\text{m}_{\text{NO}_3}} + [\text{NO}_3^-]}$$

where $f(\Delta G_{\text{rxn}}) = 1 - \exp((\Delta G_{\text{rxn}} - \Delta G_{\text{min}})/RT)$, ΔG_{rxn} = free energy of the corresponding TEAP reaction, ΔG_{min} = minimum free energy change required to drive cellular energy metabolism (-20 kJ/mol) (Schink, 1997), four parameters (μ_{max} , $K_{\text{m}_{\text{cells}}}$, $K_{\text{m}_{\text{O}_2}}$ and $K_{\text{m}_{\text{NO}_3}}$) need to be estimated while some other rate formulations need even more parameters.

The selection of the rate parameter values was based on a combination of existing information, values that could be constrained from literature or other sources of information, values that were assigned arbitrarily based on general knowledge not specific to the particular process under consideration, and fitting by trial-and-error in order to reproduce the results of the sediment slurry experiment. These rate parameters were used in the field-scale simulation without modification. The field-scale model was used to evaluate alternative initial injection strategies and design sampling frequencies and times for the first week of the injection experiment. After the first week, we expected to be able to supplement model predictions with field observations and adjust injection and sampling strategies as needed. Therefore we simulated only the first week of the experiment in the pre-experiment modeling (pre-modeling) phase. The focus for experimental design was on the primary TEAPs; uranium reduction was not considered in pre-modeling simulations.

1.3 Simulation conditions.

Fixed head boundaries are specified at $x=0$; $x= 10$ m with a hydraulic gradient of 0.03. No flow boundaries were imposed parallel to flow and at the top and bottom of the model domain. The initial concentration of extractable Fe(III) was set at 0.225 M in the fill zone, 0.15 M in the intact saprolite zone, and zero in the gravelly zone based on sediment extraction data. The initial and upstream boundary concentrations of nitrate, dissolved sulfate, and uranium were set at 0.5 mM, 0.885 mM, and 1 μM , respectively, based on pre-experimental groundwater monitoring data. The injection rate for the bromide/ethanol solution is 3.0 L/min at each of the three injection wells (total 9.0 L/min). Injected tracer and ethanol concentrations are 500 mg/L and 10 mM, respectively. The initial time step is 0.01 hour, and the maximum time step used in the simulation is 0.5 hour.

3. RESULTS AND CONCLUSION

Figure 4 shows comparisons of model predictions and observations at 2.5 m (MLS-A, MLS-B, FW216) and 7.5 m (FW202) downstream of the injection wells (see Figure 2) during the first week (7 days or 168 hours) of biostimulation. Generally, the model predictions and observations match reasonably well given that no parameter fitting was performed for the field observations. The timing and rates of utilization of the various terminal electron acceptors is approximately correct in the simulation results. The primary mismatches occur at MLSA-4 and MLSA-5, ports at which the bromide simulation very poorly matches the observed concentrations, suggesting that incorrect representation of the flow pathways (probably associated with uncharacterized physical heterogeneity) is the cause of the mismatch rather than improper modeling of the reaction system and rates. We will further refine the flow model as more data become available. Additional reactive transport simulations of the field-scale biostimulation experiment will be performed after completion of the experiment in order to gain more insight into the complex interactions between biogeochemical transformation and hydrologic flow and transport processes in structured porous media. Those simulations will include uranium reduction in addition to the primary TEAPs considered in pre-modeling simulations. In the long term, this research will lead to development of a general strategy for controlled bioremediation of metals and radionuclides in such subsurface environments.

TABLE 2. Metabolic energy-generating terminal electron-accepting processes (TEAPs)

Number	Reaction	Catalyzed By Microorganisms *
(1)	$\text{CH}_3\text{CH}_2\text{OH} + 3\text{O}_2 \rightarrow 2\text{HCO}_3^- + \text{H}_2\text{O} + 2\text{H}^+$	AM, DM
(2)	$\text{CH}_3\text{CH}_2\text{OH} + 2.4\text{NO}_3^- + 0.4\text{H}^+ \rightarrow 2\text{HCO}_3^- + 1.2\text{N}_2 + 2.2\text{H}_2\text{O}$	DM
(3)	$\text{CH}_3\text{CH}_2\text{OH} + 0.5\text{NO}_3^- \rightarrow \text{CH}_3\text{COO}^- + 0.5\text{NH}_4^+ + 0.5\text{H}_2\text{O}$	DRM1, DRM2, DRM3
(4)	$\text{CH}_3\text{CH}_2\text{OH} + 2\text{MnO}_2 + 3\text{H}^+ \rightarrow \text{CH}_3\text{COO}^- + 2\text{Mn}^{2+} + 3\text{H}_2\text{O}$	DRM2, DRM3
(5)	$\text{CH}_3\text{CH}_2\text{OH} + 4\text{FeOOH} + 7\text{H}^+ \rightarrow \text{CH}_3\text{COO}^- + 4\text{Fe}^{2+} + 7\text{H}_2\text{O}$	DRM2, DRM3
(6)	$\text{CH}_3\text{CH}_2\text{OH} + 0.5\text{SO}_4^{2-} \rightarrow \text{CH}_3\text{COO}^- + 0.5\text{HS}^- + 0.5\text{H}^+ + \text{H}_2\text{O}$	DRM3, SO4RM
(7)	$\text{CH}_3\text{CH}_2\text{OH} + 2\text{S}^0 + \text{H}_2\text{O} \rightarrow \text{CH}_3\text{COO}^- + 2\text{HS}^- + 3\text{H}^+$	DMR3, S0RM
(8)	$\text{CH}_3\text{CH}_2\text{OH} + 0.5\text{HCO}_3^- \rightarrow \text{CH}_3\text{COO}^- + 0.5\text{CH}_4 + 0.5\text{H}^+ + 0.5\text{H}_2\text{O}$	MGM
(9)	$\text{CH}_3\text{COO}^- + 2\text{O}_2 \rightarrow 2\text{HCO}_3^- + \text{H}^+$	AM, DM
(10)	$\text{CH}_3\text{COO}^- + 1.6\text{NO}_3^- + 0.6\text{H}^+ \rightarrow 2\text{HCO}_3^- + 0.8\text{N}_2 + 0.8\text{H}_2\text{O}$	DM
(11)	$\text{CH}_3\text{COO}^- + \text{NO}_3^- + \text{H}_2\text{O} + \text{H}^+ \rightarrow 2\text{HCO}_3^- + \text{NH}_4^+$	DRM2, DRM3
(12)	$\text{CH}_3\text{COO}^- + 4\text{MnO}_2 + 7\text{H}^+ \rightarrow 2\text{HCO}_3^- + 4\text{Mn}^{2+} + 4\text{H}_2\text{O}$	DRM2, DRM3
(13)	$\text{CH}_3\text{COO}^- + 8\text{FeOOH} + 15\text{H}^+ \rightarrow 2\text{HCO}_3^- + 8\text{Fe}^{2+} + 12\text{H}_2\text{O}$	DRM2, DRM3
(14)	$\text{CH}_3\text{COO}^- + \text{SO}_4^{2-} \rightarrow 2\text{HCO}_3^- + \text{HS}^-$	DRM3, SO4RM
(15)	$\text{CH}_3\text{COO}^- + 4\text{S}^0 + 4\text{H}_2\text{O} \rightarrow 2\text{HCO}_3^- + 4\text{HS}^- + 5\text{H}^+$	DRM3, S0RM
(16)	$\text{CH}_3\text{COO}^- + \text{H}_2\text{O} \rightarrow \text{HCO}_3^- + \text{CH}_4$	MGM

*DRM – Dissimilatory reducing microorganisms, AM – Aerobic microorganisms, DM – Denitrifying microorganisms, SO4RM – Sulfate reducing microorganisms, S0RM – Sulfur reducing microorganisms, MGM – methanogenic microorganisms.

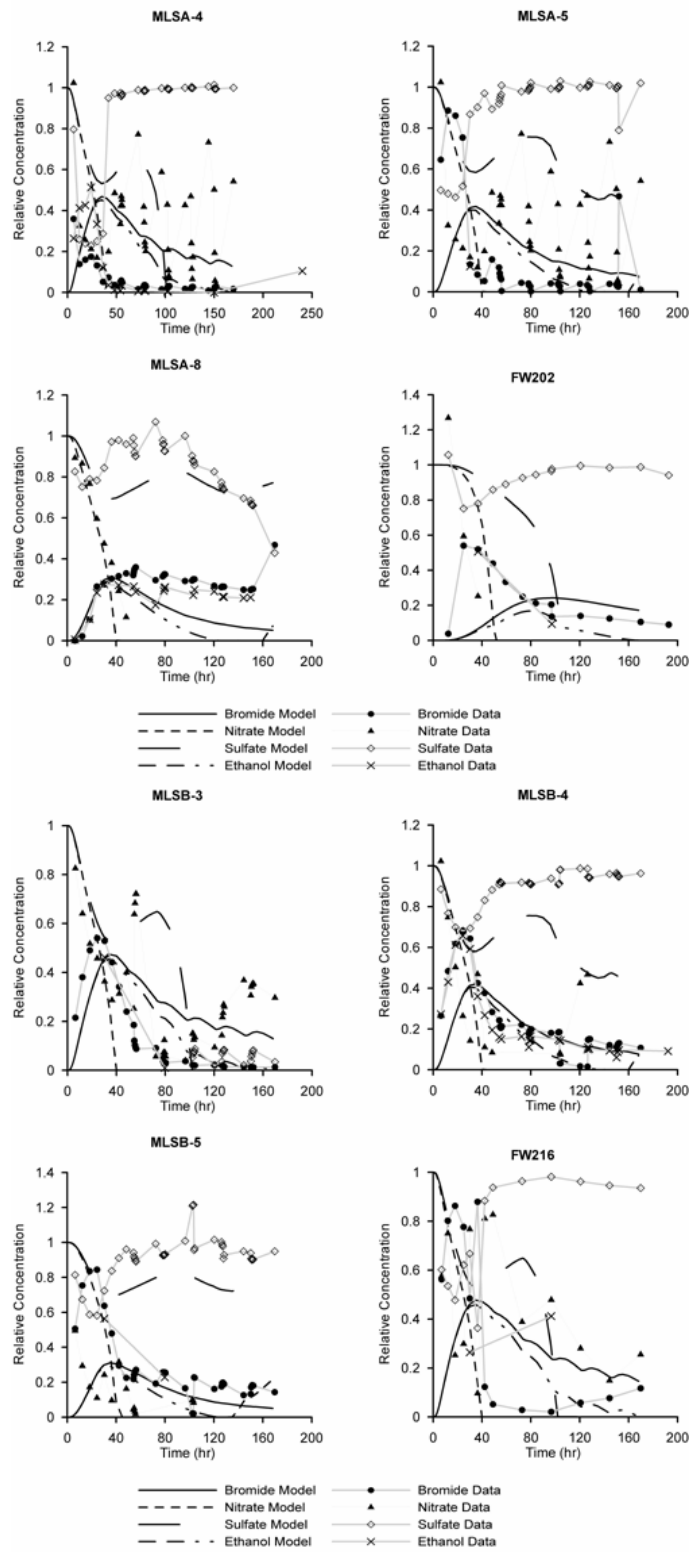


FIGURE 4. Comparisons of model predictions with observations.

REFERENCES

- Driese, S. G., L. D. McKay, and C. P. Penfield. Lithologic and pedogenic influences on porosity distribution and groundwater flow in fractured sedimentary saprolite: A new application of environmental sedimentology. *Journal of Sedimentary Research*, Vol. 71(5), 843-857, 2001.
- Fang, Y., G.T. Yeh and W.D. Burgos. A new paradigm to model reaction-based biogeochemical processes. *Water Resources Research*, 39(4), 1083-1108, 2003.
- Fang, Y., S. B. Yabusaki and G.T. Yeh. A General simulator for reaction-based biogeochemical processes, *Computers & Geosciences*, Vol 32(1), 64-72, 2005.
- McKay, L. D., S. G. Driese, K. H. Smith, and M. J. Vepraskas. Hydrogeology and pedology of saprolite formed from sedimentary rock, eastern Tennessee, USA, *Geoderma*, Vol 126(1-2), 27-45, 2005.
- Rittman, B.E. and P.L. McCarty. *Environmental Biotechnology: Principals and Applications*. New York, NY: McGraw-Hill, Boston, 754pp, 2001.
- Roden, E. E. and T. D. Scheibe. Conceptual and numerical model of uranium(VI) reductive immobilization in structured subsurface sediments. *Chemosphere*, Vol. 59(5), 617-628, 2005.
- Roden E.E., Y. Fang, T.D. Scheibe and S. Brooks. TEAPREVU: A numerical simulation model of Terminal Electron-Accepting Processes in a Representative Elementary Volume of Uranium-contaminated subsurface sediment. <http://bama.ua.edu/~eroden/BiogeochemicalModeling/TEAPREVUJan2005.pdf>, 2005.
- Roden E.E. TEAPREV: A numerical tool for assessing rates of terminal electron-accepting processes in a representative elementary volume of subsurface sediment. *Geological Society of America Abstracts with Programs*, Vol. 37, No. 7, p. 535, 2005.
- Scheibe, T. D., S. C. Brooks, W. Kamolpornwijit, Y. Fang, and E. E. Roden. Identification of physical and chemical mass transfer processes by a tracer flush experiment. *EOS Trans. AGU*, 86(18), Joint Assembly Supplement, Abstract H51A-02, 2005.
- Schink B.. Energetics of syntrophic cooperation in methanogenic degradation. *Microbiol Mol Biol Rev* 61: 262–280, 1997.
- Yeh, G-T, J. Sun, P. Jardine, W.D. Burgos, Y. Fang, M-H Li, M.D. Siegel. "HYDROGEOCHEM 5.0: a Three-Dimensional Model of Coupled Fluid Flow, Thermal Transport, and HYDROGEOCHEMical Transport through Variably Saturated Conditions - Version 5.0". ORNL/TM-2004/107 (May-2004).